DOI:10.1021/jf9014334

JOURNAL OF AGRICULTURAL AND FOOD CHEMISTRY
ARTICLE

The Human Bitter Taste Receptor hTAS2R50 Is Activated by the Two Natural Bitter Terpenoids Andrographolide and Amarogentin

Maik Behrens,[†] Anne Brockhoff,[†] Claudia Batram,[†] Christina Kuhn,[†] Giovanni Appendino,[§] and Wolfgang Meyerhof*,[†]

[†]Department of Molecular Genetics, German Institute of Human Nutrition Potsdam-Rehbruecke, Arthur-Scheunert-Allee 114−116, 14558 Nuthetal, Germany, and [§]Dipartimento di Scienze Chimiche, Università del Piemonte, Orientale, Alimentari, Farmaceutiche e Farmacologiche, Via Bovio 6, 28100 Novara, Italy

Bitterness perception in mammals is mediated through activation of dedicated bitter taste receptors located in the oral cavity. Genomic analyses revealed the existence of orthologous mammalian bitter taste receptor genes, which presumably recognize the same compounds in different species, as well as species-specific receptor gene expansions believed to fulfill a critical role during evolution. In man, 8 of the 25 bitter taste receptors (hTAS2Rs) are closely related members of such an expanded subfamily of receptor genes. This study identified two natural bitter terpenoids, andrographolide and amarogentin, that are agonists for the orphan receptor hTAS2R50, the most distant member of the subfamily. This paper presents the pharmacological characterization of this receptor and analyzes its functional relationship with the previously deorphaned hTAS2R43, hTAS2R44, hTAS2R46, and hTAS2R47. Insights into the general breadth of tuning, functional redundancies, and relationships between pharmacological activation patterns and amino acid homologies for this receptor subfamily are presented.

KEYWORDS: Bitter taste; TAS2Rs; heterologous expression; andrographolide; amarogentin

INTRODUCTION

Humans perceive the bitterness of thousands of structurally diverse compounds with specialized bitter taste receptor cells (TRCs) present in the oral cavity. Anatomically, TRCs, including those responsible for the recognition of bitter compounds, are organized in multicellular structures called taste buds. On the tongue, taste buds are embedded in three different types of taste papillae, the fungiform, foliate, and vallate papillae (*1*). Each bitter taste receptor cell expresses a subset of the 25 human bitter taste receptor genes (hTAS2Rs) (*2*). The TAS2R proteins are glycoproteins (*3*) and consist of a very short extracellular amino terminus, an intracellular carboxyl terminus, and seven transmembrane domains typical for the G protein-coupled receptor superfamily.

The perception of bitter compounds by hTAS2Rs is very important for establishing healthy diets because many pharmacologically active or even toxic plant metabolites taste bitter (*4*) and, thus, ingestion can be avoided. Hence, it is not surprising that a number of the 13 hTAS2Rs deorphaned to date respond to well-known drugs or toxins. Thus, the poisonous alkaloid strychnine, a potent glycine receptor antagonist found in the seeds of the *Strychnos nux vomica* tree, was reported to activate the three receptors hTAS2R7 (*5*), hTAS2R10 (*6*), and hTAS2R46 (*7*). A similar number of hTAS2Rs, hTAS2R14 (*5*), hTAS2R43, and hTAS2R44 (*8*), recognize the carcinogen and nephrotoxic compound aristolochic acid produced by some plant species belonging to the Aristolochiaceae family. Picrotoxinin, an antagonist of $GABA_A$ receptors, is present in the seeds of the plant *Anamirta paniculata* and activates the two receptors hTAS2R14 (*9*) and hTAS2R46 (*7*).

Clearly, during mammalian evolution contacts with particular poisonous bitter plant metabolites has not been static, but rather highly variable given the diversity of habitats and other environmental parameters, such as climatic zones and seasonal effects. Consequently, it has been reported that the bitter taste receptor repertoire differs largely across animal species, including man. As Shi and colleagues pointed out (*10*), comparison between rodent and human bitter taste receptor genes revealed the existence of one-to-one orthologous genes, perhaps mediating conserved function in rodents and man, as well as species-specific expansions of bitter taste receptor genes, which likely serve specialized functions. One such group of species-specific expansions is the human TAS2R subfamily consisting of the eight genes hTAS2R43, hTAS2R44, hTAS2R45, hTAS2R46, hTAS2R47, hTAS2R48, hTAS2R49, and hTAS2R50 (**Figure 1A**).

Cognate bitter compounds are already known for four of the eight TAS2Rs. Whereas the receptor hTAS2R46 has been reported to be very broadly tuned, responding to a wide range of sesquiterpene lactones, clerodane, and labdane diterpenoids and additional natural and artificial bitter compounds (*7*), the other three receptors seem to be more specialized and show a

*Author to whom correspondence should be addressed (telephone +49 33200 88282; fax +49 33200 88384; e-mail meyerhof@dife.de).

 Published on Web 10/09/2009

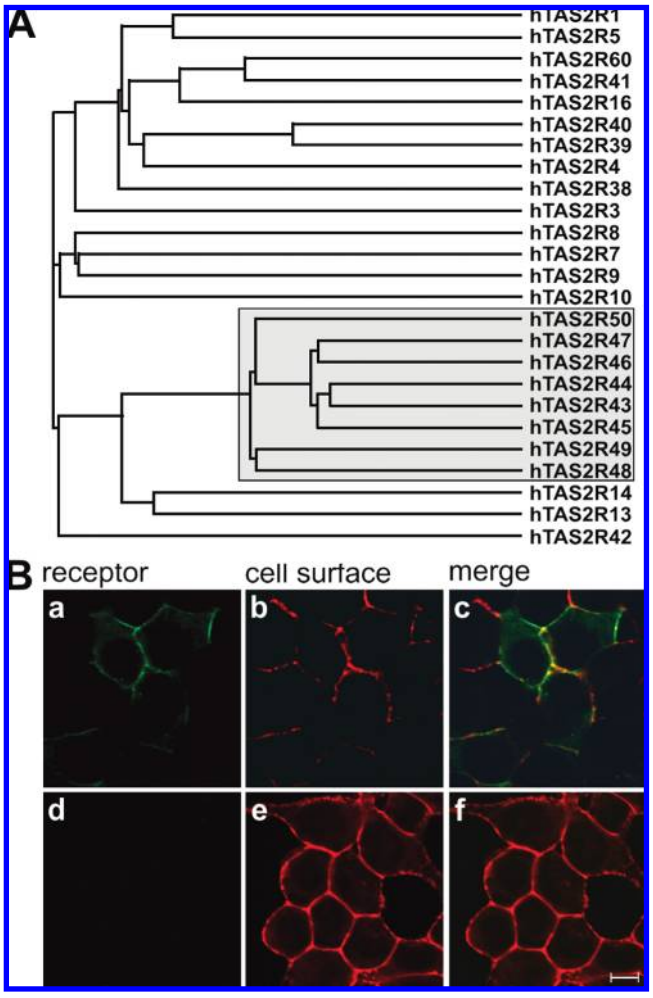

Figure 1. Cladogram of human bitter taste receptor genes and heterologous expression of hTAS2R50 in HEK 293T cells: (**A**) nucleotide sequence alignment of the coding regions of all 25 hTAS2R genes reveals a subfamily of 8 related receptors (shaded in gray); (**B**) expression of hTAS2R50 after transient transfection into HEK 293T Gα16gust44 cells. In **B**, confocal images of hTAS2R50 (a−c) and mock transfected (d−f) HEK 293T Gα16gust44 cells are shown. Receptor expression is detected by a primary antibody against the HSV-tag in combination with an Alexa488-labeled anti-mouse antibody (green). Plasma membrane is visualized by biotinylated concanavalin A binding to plasma glycoproteins in combination with streptavidin−Alexa633 (red). Receptor localization at the plasma membrane is indicated by yellow areas in the overlay (c). Scale = 8 μM.

considerable overlap in their agonist activation pattern. Thus, the receptor hTAS2R43 responds to the artificial sweeteners saccharin and acesulfame K, and the saccharin-related compounds 6-nitrosaccharin and *N*-isopropyl-2-methyl-5-nitrobenzenesulfonamide (IMNB) as well as the bitter plant metabolites aristolochic acid and aloin (*8*, *11*, *12*). The receptor most closely related to hTAS2R43, hTAS2R44, also recognizes saccharin, acesulfame K, aristolochic acid, and aloin, but is activated neither by 6-nitrosaccharin nor by IMNB (*8*, *12*). Interestingly, the receptor hTAS2R47, on the one hand, is functionally linked to hTAS2R43 by the common agonist 6-nitrosaccharin (*11*); on the other hand, it shares the agonist denatonium with hTAS2R46 (*7*).

Although half of the receptors belonging to this subfamily have been deorphaned, many open questions remain unanswered. In this context, we present here the functional characterization of the fifth and least related member of the subfamily, hTAS2R50. The deorphanization and characterization of hTAS2R50 made it possible to investigate the predominant breadth of tuning found in this hTAS2R subfamily. Moreover, comparison of the pharmacological profiles of all five deorphaned subfamily members enabled us to identify the proportion of functional redundancies and to assess whether functional similarities correlate with amino acid sequence homologies within the subfamily, which presumably played a very important role during the evolution of modern hominids.

MATERIALS AND METHODS

Taste Active Compounds. Acesulfame K, 2-acetylpyrazine, andrographolide, antipyrin, aristolochic acid, caffeic acid, chlorogenic acid, denatonium benzoate, gingkolide A, 1-naphthoic acid, nicotinic acid, phenythiocarbamide, picrotoxinin, quinine hydrochloride, resveratrol, D-(−)-salicin, strychnine (nitrate salt), theobromine, and (−)-α-thujone were ordered at the highest available purity from Sigma/Fluka (Sigma-Aldrich, Taufkirchen, Germany). Amarogentin was purchased from Chromadex (Distributor LGC Standards, Wesel, Germany). Sodium cyclamate was a gift from Dr. K. Hoppe. Isohumulone was a gift from Dr. T. Hofmann. Absinthin was available from previous studies and isolated according to procedures published recently (cf. Brockhoff et al. (2007) and Supporting Information therein (*7*)).

Bitter Receptor Constructs. The coding regions of hTAS2R genes were amplified from HEK 293 cell genomic DNA and cloned into the vector pcDNA5/FRT (Invitrogen) as before (*6*). Briefly, the receptor sequences were flanked with an amino-terminal sst-tag coding for the 45 amino-terminal amino acid residues of rat somatostatin receptor subtype 3 to improve cell membrane targeting and at the carboxy terminus with the *Herpes simplex* glycoprotein D epitope for immunological detection. The constructs of hTAS2R43, hTAS2R44, and hTAS2R46 were published previously (*7*, *8*), the cDNA used for the hTAS2R47 construct corresponds to GenBank accession no. NT_009714, and the cDNA used for hTAS2R50 corresponds to a naturally occurring variant of the receptor gene (NW_925328 with synonymous SNP at nucleotide position 777 (G777A) of the coding region; cf. Kim et al. (2005) and Supporting Information therein (*13*)).

Immunocytochemistry. For expression analysis we seeded HEK 293T Gα16gust44 cells on poly-D-lysine (10 μg/mL) coated glass coverslips into 24-well plates. Transient transfection with Lipofectamine2000 (Invitrogen) was performed according to the manufacturer's instructions. After 24 h, cells were washed with warm PBS and incubated on ice for 30 min to block endocytosis. Cell membrane was visualized by binding of biotin-conjugated concanavalin A (Sigma) to membrane glycoproteins for 1 h. After washing, cells were fixed with acetone/methanol 1:1 for 2 min on ice and washed again. To reduce unspecific binding, cells were incubated with 3% goat serum for 30 min at room temperature. Receptor proteins were detected by mouse anti-HSV antiserum (Novagen, 1:15000) at 4 °C overnight. After washing, we incubated the cells with Alexa488-conjugated goat anti-mouse antiserum (Molecular Probes, 1:2000) and streptavidin−Alexa633 (Molecular Probes, 1:1000) for 1 h at room temperature in PBS and 3% goat serum. Finally, cells were rinsed and mounted using DakoCytomation Fluorescent Mounting Medium (DAKO, Hamburg, Germany). Receptor expression was analyzed by confocal laser scanning microscopy using a Leica TCS SP2 (Leica, Bensheim, Germany).

Functional Expression of hTAS2Rs. For functional analysis HEK 293T Gα16gust44 cells were seeded into poly-D-lysine coated (10 μg/mL) 96-well plates and transfected with Lipofectamine2000 (Invitrogen) according to the manufacturer's instructions. After 24 h, cells were loaded with fluorescent dye (Fluo-4 AM, Molecular Probes, 2 μM in DMEM without serum) and incubated for at least 1 h at 37 °C. To remove residual dye, cells were washed three times with C1 buffer (130 mM NaCl, 5 mM KCl, 10 mM Hepes, pH 7.4, 2 mM $CaCl_2$, 10 mM Glucose) at room temperature. Stock solutions of test compounds were prepared in DMSO if necessary. Test compounds were diluted in C1 buffer not exceeding a final DMSO concentration of 1%. Applied maximal concentrations of test compounds were individually adjusted to avoid induction of unspecific signals in mock-transfected cells. Calcium responses of transfected cells upon test compound application were measured using a Fluorometric Imaging Plate Reader (Molecular Devices, Munich, Germany). Data were

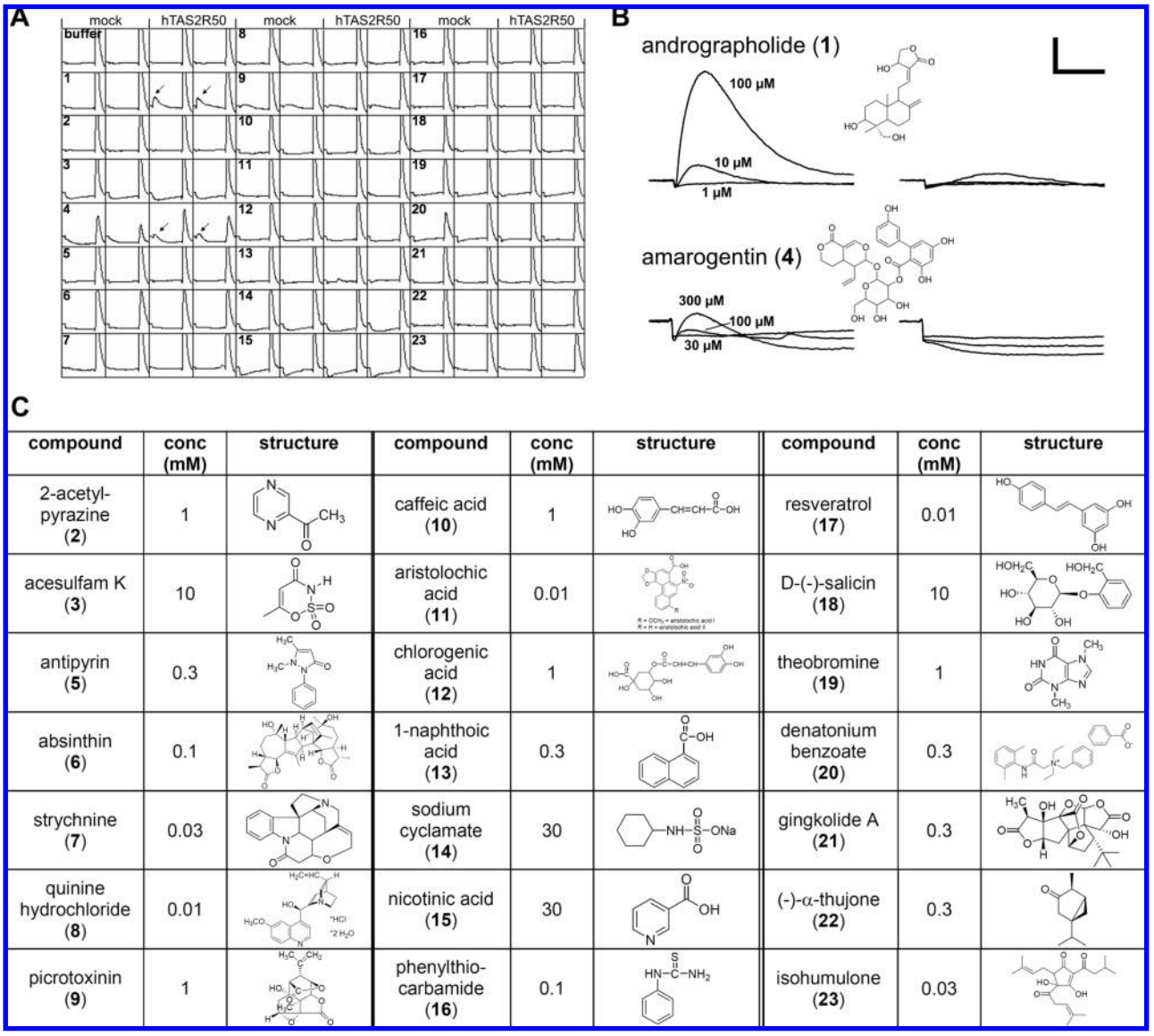

compound	conc (mM)	structure	compound	conc (mM)	structure	compound	conc (mM)	structure
2-acetyl-pyrazine (2)	1		caffeic acid (10)	1		resveratrol (17)	0.01	
acesulfam K (3)	10		aristolochic acid (11)	0.01		D-(-)-salicin (18)	10	
antipyrin (5)	0.3		chlorogenic acid (12)	1		theobromine (19)	1	
absinthin (6)	0.1		1-naphthoic acid (13)	0.3		denatonium benzoate (20)	0.3	
strychnine (7)	0.03		sodium cyclamate (14)	30		gingkolide A (21)	0.3	
quinine hydrochloride (8)	0.01		nicotinic acid (15)	30		(-)-α-thujone (22)	0.3	
picrotoxinin (9)	1		phenylthio-carbamide (16)	0.1		isohumulone (23)	0.03	

Figure 2. Screening of hTAS2R50 transfected HEK 293T cells. (**A**) Cells were transfected in duplicates either with empty expression vector (mock) or with a construct coding for hTAS2R50 (hTAS2R50). After ~24 h of incubation, cells were loaded with Fluo-4 AM, washed, and challenged with buffer (buffer) or one of 23 bitter compounds (numbered 1−23, see **B** and **C**). To control for cell viability 100 nM SST14 was applied, subsequently activating endogenous somatostatin receptors. Arrows point to increases of intracellular calcium levels of hTAS2R50 transfected cells monitored after addition of compounds **1** and **4**. Note the absence of signals in the wells containing the corresponding mock-transfected cells. (**B**) Calcium traces of hTAS2R50 (left) and mock transfected cells (right) monitored after stimulation with the indicated concentrations of andrographolide (upper panel) or amarogentin (lower panel) demonstrate the dose dependence of the cellular responses. Scale: *y*-axis, ΔF = 2000 fluorescence counts in arbitrary units; *x*-axis, 2 min. (**C**) Negative compounds used for screening of hTAS2R50. The numbers printed in bold correspond to the numbering used in **A**. Substance concentrations used for the screening are given in millimolar. Chemical structures for each compound are depicted.

collected from at least two independent experiments carried out in duplicates. For the calculation of dose−response curves, signals of two to four wells receiving the same concentration of test substances were averaged, and the fluorescence changes of corresponding mock-transfected cells were subtracted. Signals were normalized to background fluorescence. For the calculation of EC_{50} values, plots of amplitude versus concentrations were prepared in Sigma Plot. By nonlinear regression of the plots to the function $f(x) = 100/[1 + (EC_{50}/x)^{nH}]$, where x is the agonist concentration and nH is the Hill coefficient, the EC_{50} of agonist−receptor interaction was calculated.

RESULTS

Comparison of the nucleic acid sequences corresponding to the coding regions of all 25 hTAS2R genes reveals the close relationships among the receptors hTAS2R43 to hTAS2R50 (**Figure 1A**). Within this group of eight receptors, hTAS2R43, hTAS2R44, hTAS2R45, hTAS2R46, and hTAS2R47 show the highest degree of similarity, whereas hTAS2R48, hTAS2R49, and hTAS2R50 comprise more distantly related receptors. Another pair of receptors, hTAS2R13 and hTAS2R14, seem to be more remote relatives bridging the gap to the rest of the hTAS2R gene family members.

A prerequisite for the successful identification of cognate bitter substances for bitter taste receptors by heterologous expression is that the receptor proteins are present at the cell surface of the chosen cell lines. To identify whether this holds true for hTAS2R50, we transiently expressed cDNA for this receptor in HEK 293T Gα16gust44 cells. For efficient plasma membrane translocation a sequence coding for the first 45 amino acids of the rat somatostatin receptor type 3 was added in frame to the 5′-end of the expressed hTAS2R50 construct (*14*). Furthermore, a

sequence coding for the *Herpes simplex* glycoprotein D epitope (HSV-tag) for immunodetection was added in frame to the 3′-end (*6*). Twenty-four hours after transfection, cells were stained by indirect immunofluorescence with an antiserum directed against the HSV-tag and an Alexa488-labeled anti-mouse IgG to visualize the receptor protein (green) as well as with biotinylated concanavalin A, a lectin labeling carbohydrate moieties of cell surfaces (red), in combination with streptavidin−Alexa633 (**Figure 1B**). Although weak signals in cytoplasmatic regions of hTAS2R50 transfected cells are stained with the anti-HSV antibody shown in green, the majority of the receptor-specific signals were evident at the plasma membrane, where a clear overlap with the cell surface marker concanavalin A, and thus successful plasma membrane insertion, could be demonstrated (**Figure 1B**, a−c). The absence of green signals in mock-transfected cells underscores the specificity of the immunocytochemical signals (**Figure 1B**, d−f).

To identify bitter compounds activating hTAS2R50, we screened HEK 293T cells stably expressing the G protein chimera Gα16gust44, which were transiently transfected with hTAS2R50 cDNA, and performed calcium imaging analyses (**Figure 2**). The G protein subunit Gα16gust44 effectively couples TAS2Rs to the phospholipase C-mediated generation of inositol trisphosphate and elevation of cytosolic Ca^{2+} concentration (*3*, *7*−*9*, *15*, *16*). The compounds used for the screening included a number of well-known bitter compounds and published agonists for various hTAS2Rs, respectively, as well as additional substances chosen on the basis of their chemical structures and occurrence in human diets or medication. Of the 23 substances used for the screening only 2, amarogentin and andrographolide, were able to stimulate receptor-transfected cells. We used for the initial screening substance concentrations not leading to artificial calcium signals as can be seen for mock-transfected control cells that were stimulated with the same compound concentration but without receptor cDNA. The reaction of hTAS2R50 to only two substances clearly demonstrates that this receptor is another example for a rather narrowly tuned hTAS2R comparable to the subfamily members hTAS2R43 (*8*, *11*, *12*), hTAS2R44 (*8*, *12*), and hTAS2R47 (*11*) and distinct from the very broadly tuned hTAS2R46 (*7*). Additionally, the initial screening revealed almost no functionally overlapping agonist activation pattern with other hTAS2Rs. The inability to respond to strychnine functionally separates hTAS2R50 from hTAS2R7 (*5*), hTAS2R10 (*6*), and hTAS2R46 (*7*), whereas the unresponsiveness to aristolochic acid stimulation, a potent activator of hTAS2R14 (*5*), hTAS2R43, and hTAS2R44 (*8*), separates hTAS2R50 also from this group of receptors. The fact that denatonium, salicin, and phenylthiocarbamide (PTC), known agonists of hTAS2R4 (*17*), hTAS2R47 (*11*), hTAS2R16 (*6*), and hTAS2R38 (*15*, *18*), respectively, also do not activate hTAS2R50, clearly underscores its distinctiveness. Also, the most recently deorphaned human bitter taste receptors, hTAS2R1, which responds mainly to bitter amino acids and peptides (*19*), and hTAS2R9, responding to the drugs ofloxacin, procainamide, and pirenzapine (*20*), are functionally distinct from hTAS2R50. The two newly identified agonists, amarogentin and andrographolide, although belonging to the terpenoid family of natural products, are structurally very different. Amarogentin is an iridoid glycoside further decorated by a trihydroxydiphenyl acyl moiety and is considered to be the most intense bitter compound for humans (*21*). Andrographolide is the major bitter diterpenoid isolated from *Maha-tita* (King of bitters), the Ayurvedic plant *Andrographys paniculata* Nees., and was recently shown to activate hTAS2R46 as well (*7*). The observation that other glycosides and diterpenoids, such as D-(−)-salicin and gingkolide A, were included in our screening experiments and did not activate hTAS2R50 indicates that the observed agonistic properties of andrographolide and amarogentin at hTAS2R50 are structure- and not class-specific.

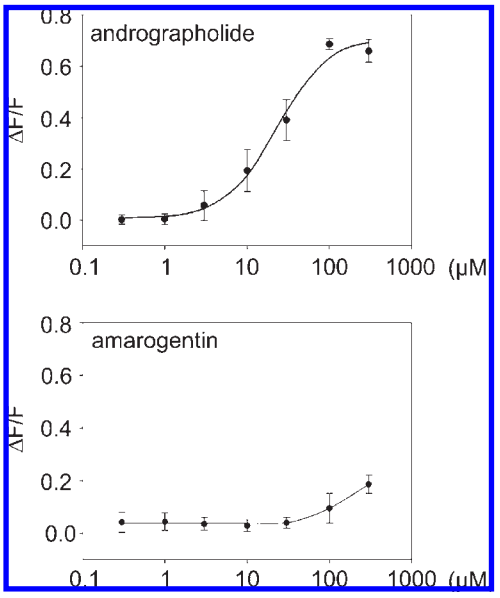

Figure 3. Dose−response relationships of andrographolide and amarogentin on activation of hTAS2R50. HEK 293T Gα16gust44 cells were transfected with hTAS2R50 cDNA. After 24 h, cells were stimulated with different concentrations of andrographolide (upper panel) and amarogentin (lower panel). Calcium responses were measured in a fluorometric imaging plate reader (FLIPR) and normalized to SST14 responses stimulating endogenous somatostatin receptors. Mean signals of three independent experiments were plotted against log agonist concentrations. Nonlinear regressions and half-maximal receptor activations (EC_{50}) were calculated using SigmaPlot2000. For andrographolide an EC_{50} value of 22.9 ± 4.9 μM was determined. As the highest artifact-free concentration used for amarogentin did not result in signal saturation, an EC_{50} value was not determined, but was estimated to be >300 μM.

Amarogentin and andrographolide that specifically activated hTAS2R50 were analyzed in more detail by monitoring their corresponding dose−response relationships (**Figure 3**). For this experiment HEK 293T Gα16gust44 cells transiently transfected with hTAS2R50 were challenged with different concentrations of the identified agonists, and standardized responses were plotted. For andrographolide, a half-maximal receptor activation (EC_{50}) was obtained at 22.9 ± 4.9 μM (**Figure 3**, upper panel). Because signal saturation was not reached at ambient concentrations, determination of an EC_{50} value was not possible for amarogentin (**Figure 3**, lower panel). The apparent difference in sensitivity of hTAS2R50 for the two agonists is further underscored by the observed threshold concentration for receptor activation. Whereas andrographolide induces significant receptor responses already at a concentration of 10 μM, a 10-fold higher concentration of amarogentin (100 μM) is required.

Next, we compared the agonist activation profiles of the five deorphanized receptors of this hTAS2R gene subfamily to assess whether the high degree in amino acid sequence relationship predicts functional redundancy or not (**Figure 4**). Of the nine compounds compiled in **Figure 4**, none activated all five receptors. The highest number of receptors activated by a single substance was obtained for amarogentin, with four receptors, followed by two substances, denatonium and andrographolide, that evoked responses of three receptors. The majority of substances stimulated two receptors, with the exception of strychnine, which activated only a single receptor, hTAS2R46. Hence, although

	67%	69%	70%	68%	100%
Compound	hTAS2R43	hTAS2R44	hTAS2R46	hTAS2R47	hTAS2R50
Absinthin	-	-	3 μM	0.1 μM	-
Acesulfame K	3100 μM*	250 μM*	-	-	-
Aloin	0.3 μM	~30 μM*	-	-	-
Amarogentin	30 μM	-	10 μM	3 μM	100 μM
Andrographolide	-	-	3 μM	30 μM	10 μM
Aristolochic acid	0.0013 μM*	0.016 μM*	-	-	-
Denatonium	300 μM	-	30 μM	0.03 μM	-
Saccharin	170 μM*	80 μM*	-	-	-
Strychnine	-	-	0.1 μM	-	-
	100%	89%	87%	80%	67%

Figure 4. Comparison of the agonist-activation patterns of the deorphaned members of the hTAS2R subfamily. The nucleic acid sequence identities of the coding regions of hTAS2R43, hTAS2R44, hTAS2R46, hTAS2R47, and hTAS2R50 to hTAS2R50 (top) or hTAS2R43 (bottom) are indicated in percent (shaded in gray). The threshold values for receptor activations by bitter compounds (left row) are listed. Asterisks indicate threshold values taken from previous publications (acesulfame K, aristolochic acid, and saccharin were taken from ref *8* and the threshold for hTAS2R44 stimulated by aloin deduced from ref *12*).

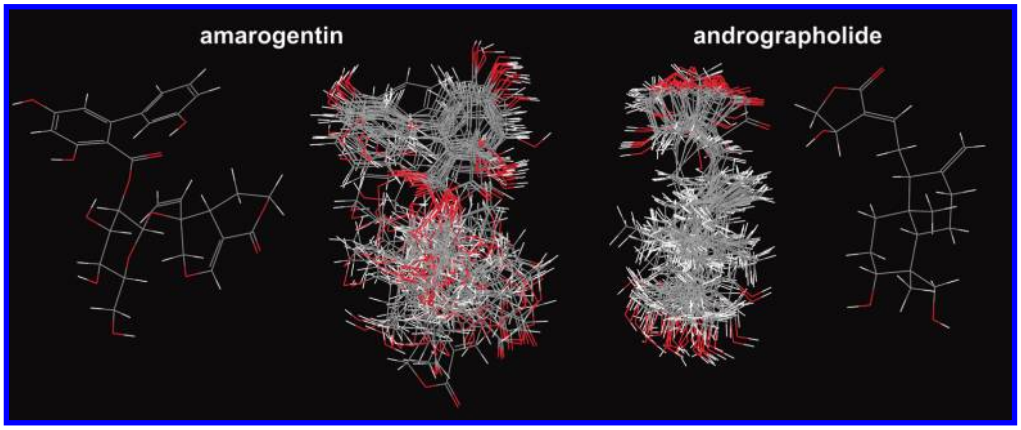

Figure 5. Conformational flexibility of amarogentin and andrographolide. The chemical structures of the two identified agonists for hTAS2R50 were analyzed using the module "Ligprep" of the Schrodinger modeling software package. The resulting conformers of each substance are depicted next to their 3D structures to visualize the conformational flexibility of hTAS2R50 agonists.

some functional redundancy is evident within this receptor subfamily, the number of shared agonists is limited. Clearly, on a functional level, hTAS2R43 and hTAS2R44 are highly related, sharing four common agonists, all of which do not activate the other three subfamily members. Although the receptor hTAS2R46, showing 87% amino acid sequence identity compared with hTAS2R43 and 85% identity compared with hTAS2R47, seems to have an intermediate relationship, it forms another functional pair with hTAS2R47 sharing four agonists as well. The two newly identified agonists for hTAS2R50, amarogentin and andrographolide, link this receptor more with the hTAS2R46/47 pair, rather than with the hTAS2R43/44 pair. However, if one extends these considerations on intrafamily functional relationships from a qualitative to a quantitative level by taking the observed threshold concentrations for the compared substances into account, the apparent degree of functional redundancy is even more reduced. If one focuses on the two newly identified substances, amarogentin and andrographolide, their recognition thresholds by the receptors hTAS2R46, hTAS2R47, and hTAS2R50 are inversely correlated. Whereas hTAS2R46 is more sensitive for andrographolide than for amarogentin (thresholds = 3 and 10 μM, respectively), hTAS2R47 instead is more sensitive to amarogentin than andrographolide (thresholds = 3 and 30 μM, respectively). Yet, hTAS2R50 is more sensitive to andrographolide than amarogentin (thresholds = 10 and 100 μM, respectively). In summary, it appears to be evident that a limited degree of functional redundancy exists within this subfamily of hTAS2Rs but that each deorphanized member exhibits a unique agonist activation pattern. Surprisingly, strychnine, which has been identified as an agonist already for three rather unrelated hTAS2Rs (hTAS2R7, hTAS2R10, and hTAS2R46 (*5*−*7*)), is the only compound not shared by any other subfamily member, exemplifying that the specificity of agonist recognition is not simply correlated with amino acid sequence homologies.

DISCUSSION

The present study identified two agonists for the previously orphan human bitter taste receptor hTAS2R50. Of the two substances, amarogentin, an intensely bitter iridoid glycoside, has not been identified to stimulate one of the hTAS2Rs published so far, whereas andrographolide, a bitter diterpenoid, was already known as an agonist for hTAS2R46 (*7*).

The two agonists are structurally very different in terms of connectivity and number of potential hydrogen donor groups, hydrogen acceptor groups, and hydrophobic sites (**Figure 5**). Consequently, in silico screening for a common pharmacophore afforded such an unmanageably large number of putative structures (not shown) to be of questionable relevance. However, the observation that the flat 2,4-dihydroxy-6-(3-hydroxyphenyl)benzoyl group was not included in any of these structures suggests that this structural element may not be critical for amarogentin binding to hTAS2R50, but rather, due to sterical hindrance, responsible for being less effective than andrographolide, for example, not leading to signal saturation (**Figure 3**). As amarogentin exhibits such an intense bitter taste, and thus resembles denatonium, another extraordinary bitter-tasting compound, structural flexibility, which is inherent to both prototypical bitter substances, might be one of the keys for the activation of multiple bitter taste receptors as evident from **Figure 4**.

Establishment of the threshold concentrations for the activation of hTAS2R50 and other hTAS2Rs belonging to the subfamily of related receptors showed that the hTAS2R50 is the most sensitive receptor for neither compound. In fact, whereas hTAS2R50 shows an intermediate sensitivity for andrographolide, it is the least sensitive of the four receptors responding to amarogentin. It seems likely that other, yet unknown, agonists might stimulate hTAS2R50 preferentially or, alternativly, that the intermediate sensitivity of this receptor is important to spread the concentration range for human bitter taste perception and achieve a better quantification of the stimuli presented. As both hTAS2R50 agonists are not particularly toxic, but even appear to exert beneficial effects, a higher sensitivity for these agonists may not have resulted in better evolutionary fitness. Amarogentin shows antileishmanial activity in hamster at doses of 2.5 mg/kg (*22*), which is approximately in the range of the threshold of the most sensitive receptor in our screen (hTAS2R47, see **Figure 4**). Similarly, andrographolide, which has been reported to exhibit antiapoptotic (*23*), anti-inflammatory (*24*, *25*), antiangiogenesis (*26*), and anticancer effects and to inhibit v-src (viral-sarcoma, an oncogenic protein tyrosine kinase), induced morphological transformation and colony formation (*27*) at concentrations close to the recognition threshold of the most sensitive receptor hTAS2R46 (**Figure 4** and ref *7*). In fact, the majority of chemicals known to stimulate hTAS2Rs cannot simply be classified as harmful, because they might even exert beneficial effects at low doses or contain toxic as well as nontoxic compounds. Examples for such compounds are aloin (hTAS2R43 and hTAS2R44 (*12*)), the cyanogenic β-glucopyranosides and the antipyretic/analgesic salicin (hTAS2R16 (*6*)), the drugs ofloxacin, procainamide, and pirenzapine, stimulating hTAS2R9 (*20*), glucosinolates, or their corresponding isothiocyanates, which are likely natural activators of hTAS2R38 (*15*, *28*), and the large number of medicinally relevant sesquiterpene lactones (hTAS2R46 (*7*)). In fact, only a few deorphaned hTAS2Rs have not been demonstrated to recognize pharmaceutically active bitter compounds, such as the denatonium responsive receptors hTAS2R4 (*17*) and hTAS2R47 (*11*), the low-affinity saccharin receptor hTAS2R8 (*12*), or hTAS2R1, which appears to be specialized to the detection of bitter peptides (*19*).

In general, human bitter taste receptors are considered to be rather broadly tuned to detect numerous compounds. The newly deorphaned receptor hTAS2R50, however, appears to be more narrowly tuned, recognizing only 2 of the set of 23 bitter tastants investigated. In this respect hTAS2R50 is similar to the other subfamily members hTAS2R43, hTAS2R44, and hTAS2R47, which also appear to be less broadly tuned specialized receptors. The hTAS2R46, on the other hand, is an exceptionally broadly tuned receptor.

As this receptor subfamily represents roughly one-third of the entire human bitter taste receptor repertoire, it is obvious that they must have been very important for human evolution. In fact, the human genome contains additional pseudogenes, which must have been part of this subfamily earlier during evolution (*10*). This and the observations of the frequent deletion of hTAS2R43 and hTAS2R45 genes from the genome of individuals (*12*), as well as the fact that the receptor gene hTAS2R46 is a segregating pseudogene containing a nonsense mutation in almost 24% of individuals, all testify to the enormous dynamic development of this subfamily (*13*). From an evolutionary standpoint, it would be highly interesting to elucidate also for the remaining orphan receptors hTAS2R45, hTAS2R48, and hTAS2R49 whether this receptor subfamily consists of mostly broadly tuned receptors. Broadly tuned receptors perhaps would better support an exploratory phase during evolution accompanied by frequent contacts to novel potentially harmful bitter plant metabolites, whereas more narrowly tuned receptors might be more important during phases of settlement in a novel environment. A third variant comes from the observation that, although every receptor of this subfamily shows a unique agonist activation pattern, which is, given the high similarities of their peptide sequences, rather astonishing, some functional redundancy can be observed. Therefore, it seems possible that these related receptors are devoted to detecting likewise related families of bitter compounds. Unfortunately, with the exception of hTAS2R46, only a handful of naturally occurring bitter agonists were identified for the other three receptors, leaving this question unanswered.

ACKNOWLEDGMENT

We thank Elke Chudoba for excellent technical assistance and Dr. Valeria D'Auria (Naples) for critically reading the manuscript.

LITERATURE CITED

(1) Miller, I. J., Jr. Anatomy of the peripheral taste system. In *Handbook of Olfaction and Gustation*; Doty, R. L., Ed.; Dekker: New York, 1995; pp 521−547.

(2) Behrens, M.; Foerster, S.; Staehler, F.; Raguse, J. D.; Meyerhof, W. Gustatory expression pattern of the human TAS2R bitter receptor gene family reveals a heterogenous population of bitter responsive taste receptor cells. *J. Neurosci.* **2007**, *27*, 12630–12640.

(3) Reichling, C.; Meyerhof, W.; Behrens, M. Functions of human bitter taste receptors depend on N-glycosylation. *J. Neurochem.* **2008**, *106*, 1138–1148.

(4) Meyerhof, W. Elucidation of mammalian bitter taste. *Rev. Physiol. Biochem. Pharmacol.* **2005**, *154*, 37–72.

(5) Sainz, E.; Cavenagh, M. M.; Gutierrez, J.; Battey, J. F.; Northup, J. K.; Sullivan, S. L. Functional characterization of human bitter taste receptors. *Biochem. J.* **2007**, *403*, 537–543.

(6) Bufe, B.; Hofmann, T.; Krautwurst, D.; Raguse, J. D.; Meyerhof, W. The human TAS2R16 receptor mediates bitter taste in response to β-glucopyranosides. *Nat. Genet.* **2002**, *32*, 397–401.

(7) Brockhoff, A.; Behrens, M.; Massarotti, A.; Appendino, G.; Meyerhof, W. Broad tuning of the human bitter taste receptor hTAS2R46 to various sesquiterpene lactones, clerodane and labdane diterpenoids, strychnine, and denatonium. *J. Agric. Food Chem.* **2007**, *55*, 6236–6243.

(8) Kuhn, C.; Bufe, B.; Winnig, M.; Hofmann, T.; Frank, O.; Behrens, M.; Lewtschenko, T.; Slack, J. P.; Ward, C. D.; Meyerhof, W. Bitter taste receptors for saccharin and acesulfame K. *J. Neurosci.* **2004**, *24*, 10260–10265.

(9) Behrens, M.; Brockhoff, A.; Kuhn, C.; Bufe, B.; Winnig, M.; Meyerhof, W. The human taste receptor hTAS2R14 responds to a variety of different bitter compounds. *Biochem. Biophys. Res. Commun.* **2004**, *319*, 479–485.

(10) Shi, P.; Zhang, J.; Yang, H.; Zhang, Y. P. Adaptive diversification of bitter taste receptor genes in mammalian evolution. *Mol. Biol. Evol.* **2003**, *20*, 805–814.

(11) Pronin, A. N.; Tang, H.; Connor, J.; Keung, W. Identification of ligands for two human bitter T2R receptors. *Chem. Senses* **2004**, *29*, 583–593.

(12) Pronin, A. N.; Xu, H.; Tang, H.; Zhang, L.; Li, Q.; Li, X. Specific alleles of bitter receptor genes influence human sensitivity to the bitterness of aloin and saccharin. *Curr. Biol.* **2007**, *17*, 1403–1408.

(13) Kim, U.; Wooding, S.; Ricci, D.; Jorde, L. B.; Drayna, D. Worldwide haplotype diversity and coding sequence variation at human bitter taste receptor loci. *Hum. Mutat.* **2005**, *26*, 199–204.

(14) Ammon, C.; Schafer, J.; Kreuzer, O. J.; Meyerhof, W. Presence of a plasma membrane targeting sequence in the amino-terminal region of the rat somatostatin receptor 3. *Arch. Physiol. Biochem.* **2002**, *110*, 137–145.

(15) Bufe, B.; Breslin, P. A.; Kuhn, C.; Reed, D. R.; Tharp, C. D.; Slack, J. P.; Kim, U. K.; Drayna, D.; Meyerhof, W. The molecular basis of individual differences in phenylthiocarbamide and propylthiouracil bitterness perception. *Curr. Biol.* **2005**, *15*, 322–327.

(16) Ueda, T.; Ugawa, S.; Yamamura, H.; Imaizumi, Y.; Shimada, S. Functional interaction between T2R taste receptors and G-protein

alpha subunits expressed in taste receptor cells. *J. Neurosci.* **2003**, *23*, 7376–7380.
(17) Chandrashekar, J.; Mueller, K. L.; Hoon, M. A.; Adler, E.; Feng, L.; Guo, W.; Zuker, C. S.; Ryba, N. J. T2Rs function as bitter taste receptors. *Cell* **2000**, *100*, 703–711.
(18) Kim, U. K.; Jorgenson, E.; Coon, H.; Leppert, M.; Risch, N.; Drayna, D. Positional cloning of the human quantitative trait locus underlying taste sensitivity to phenylthiocarbamide. *Science* **2003**, *299*, 1221–1225.
(19) Maehashi, K.; Matano, M.; Wang, H.; Vo, L. A.; Yamamoto, Y.; Huang, L. Bitter peptides activate hTAS2Rs, the human bitter receptors. *Biochem. Biophys. Res. Commun.* **2008**, *365*, 851–855.
(20) Dotson, C. D.; Zhang, L.; Xu, H.; Shin, Y. K.; Vigues, S.; Ott, S. H.; Elson, A. E.; Choi, H. J.; Shaw, H.; Egan, J. M.; Mitchell, B. D.; Li, X.; Steinle, N. I.; Munger, S. D. Bitter taste receptors influence glucose homeostasis. *PLoS ONE* **2008**, *3*, e3974.
(21) Belitz, H.-D.; Wieser, H. Bitter compounds: occurrence and structure−activity relationships. *Food Rev. Int.* **1985**, *1*, 271–354.
(22) Medda, S.; Mukhopadhyay, S.; Basu, M. K. Evaluation of the in-vivo activity and toxicity of amarogentin, an antileishmanial agent, in both liposomal and niosomal forms. *J. Antimicrob. Chemother.* **1999**, *44*, 791–794.
(23) Chen, J. H.; Hsiao, G.; Lee, A. R.; Wu, C. C.; Yen, M. H. Andrographolide suppresses endothelial cell apoptosis via activation of phosphatidyl inositol-3-kinase/Akt pathway. *Biochem. Pharmacol.* **2004**, *67*, 1337–1345.
(24) Xia, Y. F.; Ye, B. Q.; Li, Y. D.; Wang, J. G.; He, X. J.; Lin, X.; Yao, X.; Ma, D.; Slungaard, A.; Hebbel, R. P.; Key, N. S.; Geng, J. G. Andrographolide attenuates inflammation by inhibition of NF-kappa B activation through covalent modification of reduced cysteine 62 of p50. *J. Immunol.* **2004**, *173*, 4207–4217.
(25) Chiou, W. F.; Chen, C. F.; Lin, J. J. Mechanisms of suppression of inducible nitric oxide synthase (iNOS) expression in RAW 264.7 cells by andrographolide. *Br. J. Pharmacol.* **2000**, *129*, 1553–1560.
(26) Sheeja, K.; Guruvayoorappan, C.; Kuttan, G. Antiangiogenic activity of *Andrographis paniculata* extract and andrographolide. *Int. Immunopharmacol.* **2007**, *7*, 211–221.
(27) Liang, F. P.; Lin, C. H.; Kuo, C. D.; Chao, H. P.; Fu, S. L. Suppression of v-Src transformation by andrographolide via degradation of the v-Src protein and attenuation of the Erk signaling pathway. *J. Biol. Chem.* **2008**, *283*, 5023–5033.
(28) Sandell, M. A.; Breslin, P. A. Variability in a taste-receptor gene determines whether we taste toxins in food. *Curr. Biol.* **2006**, *16*, R792–794.

Received for review May 4, 2009. Accepted August 26, 2009. This work has been supported by grants from the DFG ME 1024/2-3 (W.M.) and Institute Danone (M.B.).